

# 1 Effect of vacancies on the structural and relaxor properties 2 of (Sr,Ba,Na)Nb<sub>2</sub>O<sub>6</sub>

3 Anatolii Belous, Oleg V'yunov,<sup>a)</sup> and Dmitrii Mishchuk

4 Vernadskii Institute of General and Inorganic Chemistry, 32/34 Palladina Avenue, 03680 Kyiv, Ukraine

5 Stanislav Kamba and Dmitry Nuzhnyy

6 Institute of Physics, Academy of Sciences of the Czech Republic, Na Slovance 2, 18221 Prague 8,  
7 Czech Republic

8 (Received 6 February 2007; accepted 29 May 2007)

9 It has been shown that the aliovalent substitution of sodium ions for strontium or barium ions in  
10 strontium barium niobate relaxor ferroelectric causes a decrease in vacancy content of the samples  
11 and a linear variation of unit cell volume with sodium concentration. The variation of *c* lattice  
12 parameter with sodium concentration is determined by deformations of the NbO<sub>6</sub> oxygen  
13 octahedrons in the 001 direction. Dielectric studies carried out in a wide frequency range showed  
14 that the decrease in the vacancy content of the Sr<sub>0.6-x</sub>Ba<sub>0.4</sub>Na<sub>2x</sub>Nb<sub>2</sub>O<sub>6</sub> and Sr<sub>0.6</sub>Ba<sub>0.4-y</sub>Na<sub>2y</sub>Nb<sub>2</sub>O<sub>6</sub>  
15 results in suppression of relaxor ferroelectric properties, which was manifested in both  
16 low-frequency and submillimeter region. Simultaneously, rise of the ferroelectric phase transition  
17 temperature was observed with increasing sodium concentration. © 2007 American Institute of  
18 Physics. [DOI: 10.1063/1.2752551]  
19

## 20 I. INTRODUCTION

21 The solid solutions Sr<sub>n</sub>Ba<sub>1-n</sub>Nb<sub>2</sub>O<sub>6</sub> (SBN) are formed in  
22 the concentration range of 0.2 ≤ *n* ≤ 0.8 and have a structure  
23 of so-called unfilled tetragonal tungsten bronze (TTB).<sup>1,2</sup> The  
24 SBN unit cell can be described by the general structural for-  
25 mula [(A1)<sub>2</sub>(A2)<sub>4</sub>C<sub>4</sub>][(B1)<sub>2</sub>(B2)<sub>8</sub>]O<sub>30</sub>, where A1 is the 12-  
26 coordinate site situated in the tetragonal structural channels  
27 (in the *ab* plane), A2 is the 15-coordinate site situated in  
28 pentagonal channels, and C is the 9-coordinate site situated  
29 in the triangular channels, which are vacant for SBN. A pe-  
30 culiarity of SBN structure is the distribution of strontium and  
31 barium ions between two partially vacant sites A1 and A2.  
32 The tetragonal A1 site is occupied by strontium ions only,  
33 whereas the pentagonal A2 site is statistically filled by the  
34 remaining strontium and barium ions. The degree of A-site  
35 ion disordering in the two crystallographic sites controls the  
36 electrophysical properties of SBN, in particular, the relaxor  
37 nature of the temperature dependence of permittivity  $\epsilon(T)$ .<sup>3,4</sup>  
38 Increasing the [Sr]/[Ba] ratio in SBN shifts the temperature  
39 of phase transition in the direction of lower temperatures,  
40 increases the permittivity, and enhances the relaxor proper-  
41 ties of SBN, which manifest itself by a shift of the tempera-  
42 ture of dielectric permittivity maximum with increasing  
43 frequency.<sup>1,5</sup> It should be noted that regardless of the  
44 [Sr]/[Ba] ratio, 1/6 of the A sites in the SBN structure is  
45 empty.

46 Vacancies and chemical disorder of Sr/Ba cations in the  
47 A sites of crystal lattice give rise to the creation of strong  
48 dielectric relaxation, which is responsible for the relaxor  
49 ferroelectric behavior in SBN.<sup>6</sup> Recent broadband and tera-  
50 hertz spectroscopy investigations<sup>7,8</sup> of SBN confirmed that  
51 the dielectric relaxation at 500 K has relaxation frequency in

the terahertz range just below the phonon frequencies. The  
relaxation slows down and broadens on cooling, and finally  
it splits into two components. The high-frequency one re-  
mains in the microwave range, while the low-frequency one  
is responsible for the dielectric anomaly near *T<sub>C</sub>*: it slows  
down on cooling and extremely broadens below *T<sub>C</sub>*. At the  
same time, no phonon anomalies were observed near *T<sub>C</sub>*,  
which gives evidence about the order-disorder mechanism of  
the phase transition in SBN.<sup>7</sup>

The partial aliovalent substitution of alkaline ions (for  
example, sodium) for Sr and Ba ions is one of the possibili-  
ties to control the concentration of vacancies in tetra- and  
pentagonal channels. The electroneutrality condition requires  
substitution of two Na ions for one Sr or Ba ion, which  
allows one to control the concentration of vacancies in the A  
sites.

Therefore, the goal of this work was to study the effect  
of partial aliovalent substitution of sodium ions for strontium  
or barium ions on the structure and relaxor properties of  
strontium barium niobates with the tetragonal tungsten  
bronze structure.

## II. EXPERIMENTAL METHODS

Two systems of solid solutions were investigated in the  
work: Sr<sub>0.6-x</sub>Ba<sub>0.4</sub>Na<sub>2x</sub>Nb<sub>2</sub>O<sub>6</sub> (0 ≤ 2*x* ≤ 0.3) and  
Sr<sub>0.6</sub>Ba<sub>0.4-y</sub>Na<sub>2y</sub>Nb<sub>2</sub>O<sub>6</sub> (0 ≤ 2*y* ≤ 0.2). Extra pure Nb<sub>2</sub>O<sub>5</sub>,  
BaCO<sub>3</sub>, SrCO<sub>3</sub>, and Na<sub>2</sub>CO<sub>3</sub> were used as starting reagents.  
After heat treatment of Nb<sub>2</sub>O<sub>5</sub> at 850 °C, BaCO<sub>3</sub> and SrCO<sub>3</sub>  
at 400 °C, and Na<sub>2</sub>CO<sub>3</sub> at 200 °C, required amounts of re-  
agents were weighed using a VLP-200 balance, mixed and  
homogenized using a GKML-16 vibrating mill (Hungary).  
Agate drums, chalcedony balls, and acetone as dispersed liq-  
uid were used during milling. Thermal analysis was carried  
out using a Q-1000 derivatograph (MOM Co., Orion, Hun-  
gary). Materials were synthesized at 1100–1200 °C, re-

<sup>a)</sup>Electronic mail: vyunov@ionc.kar.net

86 ground in water, dried, and homogenized. A plasticizer was  
87 added to the powders, which were then pressed into disks  
88 and sintered in a temperature range of 1300–1350 °C.

89 X-ray powder diffraction (XRPD) data were collected on  
90 a DRON-4-07 diffractometer (Cu  $K\alpha$  radiation, 40 kV,  
91 20 mA). The structure parameters were refined by the  
92 Rietveld full-profile analysis. XRD patterns were collected in  
93 the range  $2\Theta = 10\text{--}150^\circ$  in step-scan mode with a step size of  
94  $\Delta 2\Theta = 0.02^\circ$  and a counting time of 10 s per data point. As  
95 external standards, we used  $\text{SiO}_2$  ( $2\Theta$  standard) and  $\text{Al}_2\text{O}_3$   
96 (NIST SRM1976 intensity standard<sup>9</sup>).

97 Permittivity  $\epsilon$  and dielectric losses  $\tan \delta$ , were measured  
98 in a range from  $10^5$  to  $10^6$  Hz using a Tesla BM560 Q meter  
99 and at  $10^9$  Hz using the coaxial line method. For measure-  
100 ment we used the cylindrical samples, 2 mm in diameter and  
101 2 mm in thickness. The electrodes were made from silver  
102 paste by firing.

103 Measurements at terahertz frequencies from  
104 3 to  $30\text{ cm}^{-1}$  (0.09–0.9 THz) were performed in the trans-  
105 mission mode using a time-domain terahertz spectrometer  
106 based on an amplified femtosecond laser system. Two ZnTe  
107 crystal plates were used to generate (by optic rectification)  
108 and to detect (by electro-optic sampling) the terahertz pulses.  
109 Both the transmitted field amplitude and phase shift were  
110 simultaneously measured; this allowed us to determine di-  
111 rectly the complex dielectric response  $\epsilon^*(\omega) = \epsilon(\omega) - i\epsilon''(\omega)$ .  
112 For sample heating up to 900 K, we used an adapted com-  
113 mercial high-temperature cell (SPECAC P/N 5850) with  
114 1 mm thick sapphire windows.

### 115 III. RESULTS AND DISCUSSION

116 The phase changes occurring during the synthesis of  
117  $\text{Sr}_{0.6-x}\text{Ba}_{0.4}\text{Na}_{2x}\text{Nb}_2\text{O}_6$  and  $\text{Sr}_{0.6}\text{Ba}_{0.4-y}\text{Na}_{2y}\text{Nb}_2\text{O}_6$  systems  
118 by solid-state reaction technique were studied for  $2x\{2y\}$   
119  $= 0.2$ , which corresponds to the solid solutions  
120  $\text{Sr}_{0.5}\text{Ba}_{0.4}\text{Na}_{0.2}\text{Nb}_2\text{O}_6$  and  $\text{Sr}_{0.6}\text{Ba}_{0.3}\text{Na}_{0.2}\text{Nb}_2\text{O}_6$ . XRPD and  
121 thermal analysis showed that the product is formed via the  
122 following intermediate compounds:  $\text{NaNbO}_3$ ,  $\text{Ba}_5\text{Nb}_4\text{O}_{15}$ ,  
123  $\text{Sr}_3\text{Nb}_4\text{O}_{15}$ ,  $\text{BaNb}_2\text{O}_6$ ,  $\text{SrNb}_2\text{O}_6$ , and  $\text{Ba}_2\text{NaNb}_5\text{O}_{15}$ . This in-  
124 formation allowed us to optimize the synthesis conditions  
125 using  $\text{NaNbO}_3$ ,  $\text{BaNb}_2\text{O}_6$ , and  $\text{SrNb}_2\text{O}_6$  as solid-state precur-  
126 sors. The investigations enabled us to conclude that the solid  
127 solutions  $\text{Sr}_{0.6-x}\text{Ba}_{0.4}\text{Na}_{2x}\text{Nb}_2\text{O}_6$  and  $\text{Sr}_{0.6}\text{Ba}_{0.4-y}\text{Na}_{2y}\text{Nb}_2\text{O}_6$   
128 with TTB structure and space group  $Pb4m$  are formed in a  
129 wide range of  $x$  values. When the sodium content is in-  
130 creased [ $2x(2y) \geq 0.3$ ], an additional phase  $\text{Na}_3\text{NbO}_4$  ap-  
131 pears.

132 The structural parameters of polycrystalline samples of  
133 the  $\text{Sr}_{0.6-x}\text{Ba}_{0.4}\text{Na}_{2x}\text{Nb}_2\text{O}_6$  system are listed in Tables I and  
134 II. The ion positions of the  $\text{Sr}_{0.61}\text{Ba}_{0.39}\text{Nb}_2\text{O}_6$  structure,  
135 which were reported in Ref. 10, were used as initial values.

136 The unit cell parameters of the solid solutions  
137  $\text{Sr}_{0.6-x}\text{Ba}_{0.4}\text{Na}_{2x}\text{Nb}_2\text{O}_6$  and  $\text{Sr}_{0.6}\text{Ba}_{0.4-y}\text{Na}_{2y}\text{Nb}_2\text{O}_6$  as a func-  
138 tion of sodium content are shown in Fig. 1. The unit cell  
139 volume of the solid solutions  $\text{Sr}_{0.6-x}\text{Ba}_{0.4}\text{Na}_{2x}\text{Nb}_2\text{O}_6$  and  
140  $\text{Sr}_{0.6}\text{Ba}_{0.4-y}\text{Na}_{2y}\text{Nb}_2\text{O}_6$  varies linearly with sodium content  
141 and obeys Vegard's law. With increasing sodium content, the

$a$  parameter decreases in both systems, while the  $c$  parameter  
decreases in the  $\text{Sr}_{0.6}\text{Ba}_{0.4-y}\text{Na}_{2y}\text{Nb}_2\text{O}_6$  system and increases  
in the  $\text{Sr}_{0.6-x}\text{Ba}_{0.4}\text{Na}_{2x}\text{Nb}_2\text{O}_6$  system.

The  $a$  parameter decreases due to a decrease in the av-  
erage ionic radius  $\bar{R}$  in pentagonal channels ( $\bar{R} = \alpha R_{\text{Sr}}$   
 $+ \beta R_{\text{Ba}}$ , where  $\alpha$  and  $\beta$  are the molar fractions of Sr and Ba,  
respectively). In the systems  $\text{Sr}_{0.6-x}\text{Ba}_{0.4}\text{Na}_{2x}\text{Nb}_2\text{O}_6$  and  
 $\text{Sr}_{0.6}\text{Ba}_{0.4-y}\text{Na}_{2y}\text{Nb}_2\text{O}_6$ , this decrease occurs due to a de-  
crease in the 4c-site occupation by strontium and barium,  
respectively (see Tables I and II). In the system  
 $\text{Sr}_{0.6-x}\text{Ba}_{0.4}\text{Na}_{2x}\text{Nb}_2\text{O}_6$ , the  $c$  parameter increases due to the  
elongation of the  $\text{NbO}_6$  oxygen octahedrons in the [001] di-  
rection (see Table I), which is accompanied by Nb displace-  
ment from the centrosymmetrical position in the oxygen oc-  
tahedron and by an increase in the acentricity of  $\text{NbO}_6$   
octahedrons.<sup>2</sup> In the  $\text{Sr}_{0.6}\text{Ba}_{0.4-y}\text{Na}_{2y}\text{Nb}_2\text{O}_6$  system, in con-  
trast to  $\text{Sr}_{0.6-x}\text{Ba}_{0.4}\text{Na}_{2x}\text{Nb}_2\text{O}_6$ , the  $c$  parameter decreases due  
to the reduced elongation of oxygen octahedrons in the 001  
direction and lower acentricity of the  $\text{NbO}_6$  octahedrons (see  
Table II).

The increase of sodium content from  $2x(2y)=0$  to  
 $2x(2y)=0.2$  results in the redistribution of site occupation in  
the tetragonal and pentagonal channels: namely, the occupa-  
tion of the double sites in the tetragonal channels increases  
from 0.71 to 1.15 (1.02), while the occupation of the fourfold  
sites in the pentagonal channels decreases from 0.89 to 0.79  
(0.86) (see Tables I and II). The comparison of our experi-  
mental and calculated values of site occupancy in the tetrag-  
onal and pentagonal channels allows the conclusion to be  
drawn that sodium enters the tetragonal channels and that  
positive charge is compensated in the pentagonal channels by  
the decrease in strontium (barium) content.

Dielectric characteristics of  $\text{Sr}_{0.6-x}\text{Ba}_{0.4}\text{Na}_{2x}\text{Nb}_2\text{O}_6$  and  
 $\text{Sr}_{0.6}\text{Ba}_{0.4-y}\text{Na}_{2y}\text{Nb}_2\text{O}_6$  ( $\epsilon$ ,  $\tan \delta$ ) in the frequency range of  
 $10^5\text{--}10^9$  Hz are shown in Fig. 2. The composition without  
sodium,  $\text{Sr}_{0.6}\text{Ba}_{0.4}\text{Nb}_2\text{O}_6$  [ $2x(2y)=0$ ], is characterized by a  
considerable relaxation of permittivity (Fig. 2). In this case,  
the maximum of permittivity  $\epsilon_{\text{max}}$  shifts by 30 K in the fre-  
quency range studied. Regardless of whether barium or  
strontium ions are substituted, the frequency shift in  $\epsilon_{\text{max}}(T)$   
decreases with the increase in the sodium content due to the  
decrease in the A-site vacancy content. One can see that the  
cation vacancy content has larger influence on the relaxor  
properties than the  $[\text{Sr}]/[\text{Ba}]$  ratio, which was investigated in  
Refs. 3 and 4. It is clear from Fig. 2 that the decrease in the  
cation vacancy content is accompanied by a reduction of the  
relaxor ferroelectric properties. Temperature of  $\epsilon_{\text{max}}$  is no  
more frequency dependent for  $2x=0.2$  (or  $2y=0.1$ ), only the  
values of  $\epsilon_{\text{max}}$  decrease with increasing frequency, which is  
typical for diffuse or order-disorder phase transitions, where  
the relaxation frequency lies slightly above the measured fre-  
quency range. The Ba substitution with Na has stronger in-  
fluence on the suppression of relaxor properties than Sr sub-  
stitution because the concentration  $2y=0.1$  has the same  
influence on  $\Delta T_{\text{max}}$  as  $2x=0.2$ .

We fitted the frequencies  $f$  and temperatures  $T_m$  of the  
permittivity maxima in Fig. 2 using the Vogel-Fulcher  
equation,<sup>11</sup>

AQ:
#4

TABLE I. Crystallographic parameters of samples of the Sr0.6-xBa0.4Na2xNb2O6 system.

Table with 5 columns: Parameter, Sr0.6Ba0.4Nb2O6, Sr0.57Ba0.4Na0.06Nb2O6, Sr0.55Ba0.4Na0.1Nb2O6, Sr0.5Ba0.4Na0.2Nb2O6. Rows include Unit cell parameters, Ion positions, Site occupancies, Agreement factors, and Some interionic distances.

The structure parameters were refined for sodium-containing compositions only; for composition without sodium (x=0), data from Ref. 10 were taken.
Positions: 2a (0 0 Z), 2b (0 1/2 Z), and 4c (X 1/2+X Z).

200 f = f0 exp [ - Ea / (kB(Tm - TVF)) ] (1)

201 where f0 is the attempt frequency for an ion jump (f0
202 ≈ 10^13 Hz), Ea is the activation energy of permittivity relax-
203 ation, kB is the Boltzmann constant, and TVF means the freez-
204 ing (Vogel-Fulcher) temperature. Figure 3 shows the so-

called Vogel-Fulcher plot of ln f(Tm-TVF). From the fits we 205
obtained the following parameters for 2x(2y)=0 ceramic 206
SBN sample: Ea=0.060±0.022 eV and TVF=320±15 K. 207
For the ceramics with 2x=0.1, we obtained Ea 208
=0.025±0.010 eV and TVF=410±6 K. In both cases, f0 was 209
fixed at 1 × 10^13 Hz. It was quite difficult to perform the fit 210
just from three Tm temperatures, but the fitting parameters 211

TABLE II. Crystallographic parameters of samples of the Sr0.6Ba0.4-yNa2yNb2O6 system.

Table with 4 columns: Parameter, Sr0.6Ba0.4Nb2O6, Sr0.6Ba0.35Na0.1Nb2O6, and Sr0.6Ba0.3Na0.2Nb2O6. Rows include unit cell parameters (a, c, V, Px ray), ion positions (Nb1, Nb2, Na/Sr1, Ba/Sr2, O1, O2, O3, O4, O5), site occupancies (tetragonal and pentagonal channels), agreement factors (RB, RF), and interionic distances (Nb1-O4, Nb1-O4, Nb2-O5, Nb2-O5). It also includes acentricity of Nb1 and Nb2 octahedra.

The structure parameters were refined for sodium-containing compositions only; for composition without sodium (x=0), data from Ref. 10 were taken.
Positions: 2a (0 0 Z), 2b (0 1/2 Z), and 4c (X 1/2+X Z).

are quite physically reasonable. One can see that with increasing Na concentration, TVF increases and Ea decreases. It is worth noting that in samples with 2x=0.2 and with 2y ≥ 0.1, there is no shift of Tm with frequency (i.e., the relaxor behavior disappears).
The alkaline ions often make contribution to the low-frequency mechanism of polarization, while in the micro-

wave range their contribution is often insignificant.
Therefore, we considered it expedient to ascertain whether the decrease in the vacancy content due to introducing sodium ions in TTB structure affects the relaxor properties in the submillimeter wave range (terahertz) or it is a low-frequency effect only. The dielectric properties of samples of the Sr0.6-xBa0.4Na2xNb2O6 system were investigated in the



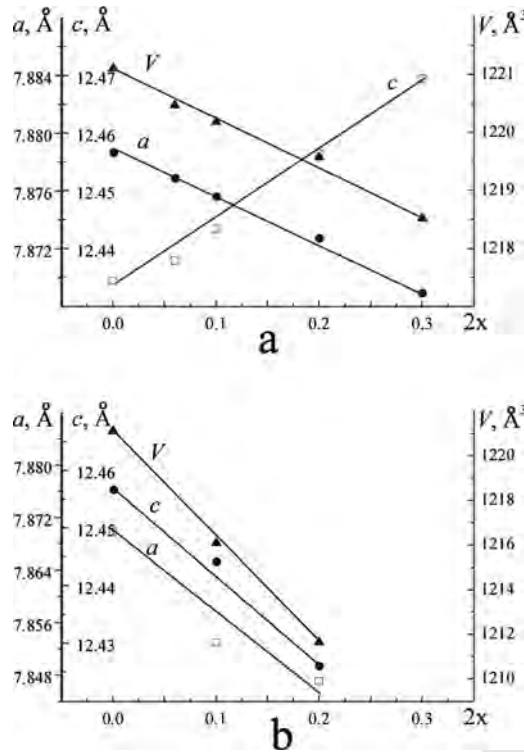


FIG. 1. Unit cell parameters of samples of the  $\text{Sr}_{0.6-x}\text{Ba}_{0.4}\text{Na}_{2x}\text{Nb}_2\text{O}_6$  (a) and  $\text{Sr}_{0.6}\text{Ba}_{0.4-y}\text{Na}_{2y}\text{Nb}_2\text{O}_6$  (b) systems as a function of sodium content.

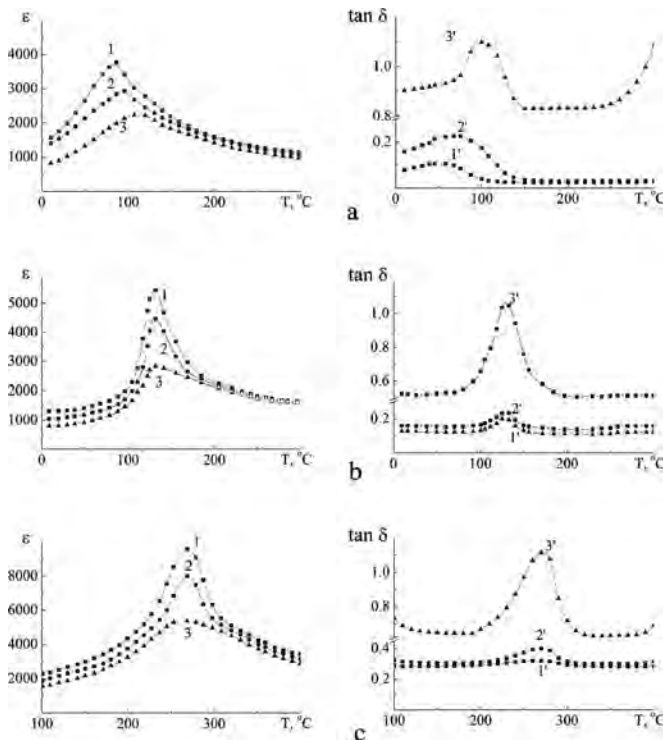


FIG. 2. Permittivity (1–3) and dielectric losses (1'–3') for samples  $\text{Sr}_{0.6}\text{Ba}_{0.4}\text{Nb}_2\text{O}_6$ ,  $2x(2y)=0$  (a),  $\text{Sr}_{0.6}\text{Ba}_{0.4-y}\text{Na}_{2y}\text{Nb}_2\text{O}_6$ ,  $2y=0.1$  (b), and  $\text{Sr}_{0.6-x}\text{Ba}_{0.4}\text{Na}_{2x}\text{Nb}_2\text{O}_6$ ,  $2x=0.2$  (c). Values were measured at  $10^5$  Hz (1, 1'),  $10^6$  Hz (2, 2'), and  $10^9$  Hz (3, 3').

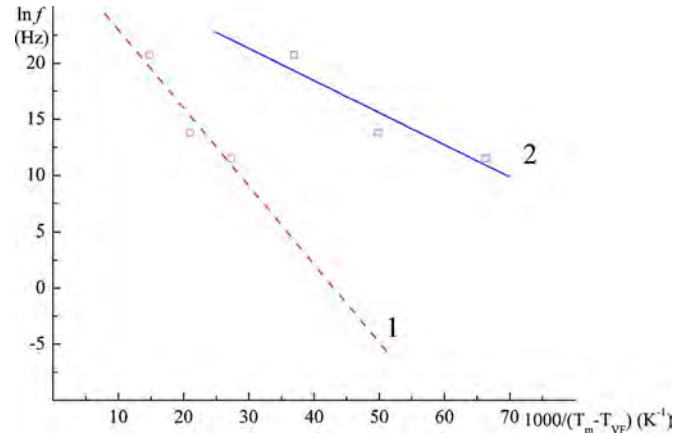


FIG. 3. (Color online) Vogel-Fulcher plots of frequencies and temperatures of the permittivity maxima for the  $\text{Sr}_{0.6-x}\text{Ba}_{0.4}\text{Na}_{2x}\text{Nb}_2\text{O}_6$  system.

terahertz frequency range. Results of these investigations for 226 samples with  $2x=0$  and  $2x=0.2$  are presented at various tem- 227 peratures in Figs. 4(a) and 4(b). We have investigated also 228 samples with  $2x=0.06$  and  $2x=0.1$ , but the results are not 229 presented here. Nevertheless, the shape of the spectra is the 230 same for all the sample compositions: permittivity  $\epsilon$  de- 231 creases with frequency, and dielectric loss  $\epsilon''$  is rather high. 232 This indicates a dielectric relaxation in the terahertz fre- 233 quency range. Both  $\epsilon$  and  $\epsilon''$  increase on heating to  $T_m$  or  $T_C$ , 234 and then they decrease on further heating. This indicates 235 slowing down of the dielectric relaxation on cooling. The 236 relaxation frequency is above  $25\text{ cm}^{-1}$  at 900 K and slows 237 down on reducing temperature to our terahertz frequency 238 range. Below  $T_m$  ( $T_C$ ) the relaxation frequency slows below 239 this range (to microwave or lower frequency range); there- 240 fore the terahertz values of both  $\epsilon$  and  $\epsilon''$  decrease on cooling 241 below  $T_m$  ( $T_C$ ). The presence of dielectric relaxation mani- 242 fests an order-disorder type of the phase transitions in all the 243 samples. Low-frequency terahertz permittivity is much 244 higher in the  $2x=0$  sample than in the  $2x=0.2$  ceramic be- 245

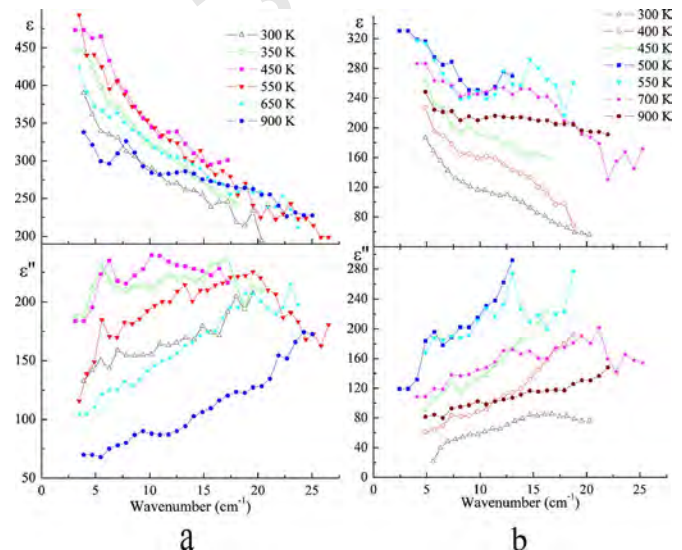


FIG. 4. (Color online) Terahertz complex dielectric spectra of  $\text{Sr}_{0.6-x}\text{Ba}_{0.4}\text{Na}_{2x}\text{Nb}_2\text{O}_6$  ceramics with (a)  $2x=0$  and (b)  $2x=0.2$ . The open and filled symbols denote temperatures below and above  $T_C$ , respectively.

cause the dielectric strength ( $\Delta\epsilon$ ) of relaxation is much higher in the undoped sample. This indicates that each Sr substitution by 2Na cations reduces the disorder in the crystal lattice due to the reduction of the vacancy concentration. It is well known that the relaxor ferroelectric behavior (i.e., the shift of permittivity peaks with measured frequency) occurs as a consequence of anomalous broadening of the distribution of relaxation frequencies on cooling.<sup>14,15</sup> This effect in pure SBN was recently experimentally confirmed.<sup>7,8</sup> Na doping of SBN reduces the vacancy concentration and therefore also random fields, which are responsible for the broad distribution of relaxation frequencies in relaxor SBN. Distribution of relaxation frequencies dramatically decreases with Na concentration, and therefore the relaxor ferroelectric behavior disappears in samples with higher Na concentration, and the sample exhibits only classical order-disorder phase transition with critical relaxation starting in the terahertz range (at high temperatures), which slows down to the megahertz range near  $T_C$ . It is worth noting that the relaxation remains in the terahertz spectra of SLTN up to the highest measured temperature 900 K, while it disappears in lead-based perovskite relaxor ferroelectrics above 600–700 K, i.e., above the Burns temperature (600–700 K), where the polar clusters disappear.<sup>16</sup> It seems to be the only difference between perovskite relaxors and our SBN relaxor system. This is presumably connected with the intrinsic (single particle) disorder in the SBN lattice at high temperatures which produces dielectric relaxations without any need of polar nanoregions. For that reason it might be quite a hard problem to estimate in the SBN the Burns temperature, where the single particle relaxation changes into a collective relaxation of polar nanoregions.

#### IV. CONCLUSION

It has been found that the formation of the  $\text{Sr}_{0.6-x}\text{Ba}_{0.4}\text{Na}_{2x}\text{Nb}_2\text{O}_6$  and  $\text{Sr}_{0.6}\text{Ba}_{0.4-y}\text{Na}_{2y}\text{Nb}_2\text{O}_6$  solid solutions is a multistage process involving the following intermediate phases:  $\text{NaNbO}_3$ ,  $\text{Ba}_5\text{Nb}_4\text{O}_{15}$ ,  $\text{Sr}_5\text{Nb}_4\text{O}_{15}$ ,  $\text{BaNb}_2\text{O}_6$ ,  $\text{SrNb}_2\text{O}_6$ , and  $\text{Ba}_2\text{NaNb}_5\text{O}_{15}$ . It has been shown that the aliovalent substitution of sodium ions for strontium or barium ions, which is accompanied by a decrease in the vacancy

content, causes a linear variation of unit cell volume in the entire  $x$  range investigated ( $0 \leq 2x \leq 0.3$ ). The variation of the  $c$  lattice parameter with  $x$  is determined by deformations of the  $\text{NbO}_6$  oxygen octahedra in the  $[001]$  direction. The investigations carried out in a wide frequency range showed that the decrease of the vacancy content in the  $\text{Sr}_{0.6-x}\text{Ba}_{0.4}\text{Na}_{2x}\text{Nb}_2\text{O}_6$  and  $\text{Sr}_{0.6}\text{Ba}_{0.4-x}\text{Na}_{2x}\text{Nb}_2\text{O}_6$  systems due to partial substitution of sodium ions for strontium or barium ions results in suppression of relaxor properties, which is observed both in the low-frequency and submillimeter range. It was also shown that the barium substitution by sodium suppresses the relaxor properties more effectively than in the case of the strontium substitution.

#### ACKNOWLEDGMENTS

The work has been supported by The Science and Technology Center in Ukraine (Project No. 3898) and the Grant Agency of the Czech Republic (Project No. 202/06/0403). The authors thank J. Petzelt for critical reading of the manuscript.

- <sup>1</sup>M.-S. Kim, P. Wang, J.-H. Lee, J.-J. Kim, H. Y. Lee, and S.-H. Cho, *Jpn. J. Appl. Phys., Part 1* **41**, 7042 (2002). 305
- <sup>2</sup>T. S. Chernaya, B. A. Maksimov, T. R. Volk, L. I. Ivleva, and V. I. Simonov, *Solid Solutions Physics of the Solid State* **42**, 1716 (2000). 306
- <sup>3</sup>L. E. Cross, *Ferroelectrics* **76**, 241 (1987). 307
- <sup>4</sup>J. R. Oliver, R. R. Neurgaonkar, and L. E. Cross, *J. Appl. Phys.* **64**, 37 (1988). 308 AQ: #2
- <sup>5</sup>J. G. Carrio, Y. P. Mascarenhas, W. Yelon, I. A. Santos, D. Garcia, and J. A. Eiras, *Mater. Res.* **5**, 57 (2002). 309
- <sup>6</sup>W. Kleemann, J. Dec, P. Lehnen, R. Blinc, B. Zalar, and R. Pankrath, *Europhys. Lett.* **57**, 14 (2002). 310
- <sup>7</sup>E. Buixaderas, M. Savinov, M. Kempa, S. Veljko, S. Kamba, J. Petzelt, R. Pankrath, and S. Kapphan, *J. Phys.: Condens. Matter* **17**, 653 (2005). 311
- <sup>8</sup>J. Banys, J. Macutkevicius, R. Grigalaitis, and W. Kleemann, *Phys. Rev. B* **72**, 024106 (2005). 312
- <sup>9</sup>Certificate of Analysis, Standard Reference Material 1976, Instrument Sensitivity Standard for X-ray Powder Diffraction (National Institute of Standards and Technology, Gaithersburg, 1991), p. 4. 313
- <sup>10</sup>T. Woike *et al.*, *Acta Crystallogr., Sect. B: Struct. Sci.* **59**, 28 (2003). 314
- <sup>11</sup>S. Kamba *et al.*, *Phys. Rev. B* **66**, 054106 (2002). 315
- <sup>12</sup>A. G. Belous, *Theor. Exp. Chem.* **34**, 331 (1998). 316
- <sup>13</sup>A. G. Belous, *J. Eur. Ceram. Soc.* **21**, 2717 (2001). 317
- <sup>14</sup>D. Viehland, M. Wuttig, and L. E. Cross, *Ferroelectrics* **120**, 71 (1991). 318
- <sup>15</sup>S. Kamba *et al.*, *J. Phys.: Condens. Matter* **12**, 497 (2000). 319
- <sup>16</sup>V. Bovtun, S. Veljko, S. Kamba, J. Petzelt, S. Vakhrushev, Y. Yakymenko, K. Brinkman, and N. Setter, *J. Eur. Ceram. Soc.* **26**, 2867 (2006). 320 AQ: #3

**AUTHOR QUERIES — 091713JAP**

- #1 Au: PLEASE DEFINE “SLNT” IF POSSIBLE.
- #2 Au: PLEASE SUPPLY FULL JOURNAL TITLE, CODEN, AND/OR ISSN IN REF. 2.
- #3 Au: PLEASE CHECK CHANGES IN REF. 9.
- #4 Au: PLEASE CHECK CHANGES IN TABLE I.
- #5 Au: PLEASE CHECK CHANGES IN TABLE II.

PROOF COPY 091713JAP